Energy 202 (2020) 117797

Contents lists available at ScienceDirect

Energy

journal homepage: www.elsevier.com/locate/energy

Operation of pumped storage hydropower plants through optimization for power systems

Gonzalo E. Alvarez

INGAR/CONICET-UTN, Instituto de Desarrollo y Diseño, Avellaneda 3657, S3000, Santa Fe, Argentina

ARTICLE INFO

Article history:
Received 18 July 2019
Received in revised form
24 April 2020
Accepted 3 May 2020
Available online 8 May 2020

Keywords:
Mixed integer linear programming
Rio grande and los reyunos hydropower plants
Hydraulic head
Pumped and discharged curves

ABSTRACT

Worldwide, there is an increase in the number of energy storage systems that are installed as a result of several benefits. These systems bring uniformity and efficiency improvements to electrical grids by storing and returning energy to the grid. They help with the integration of the new renewable energy sources, mitigating the intermittency of these sources, which is the main problem to implement them on a large scale. One of the most widespread kinds of these systems is the Pumped Storage Hydropower Plant, with an installed power capacity of 153 GW at global level. This work presents a new Mixed Integer Linear Programming model to operate these plants by maximizing the received profits. The model is distinguished from others because it allows the inclusion of a greater number of breakpoints, which means that more realistic solutions can be obtained by reducing the computational effort. To prove the usefulness of the formulation, two real plants located in Argentine Republic are tested: Rio Grande and Los Reyunos power plants which have a total installed power capacity of 975 MW. Results indicate that the proposed model reaches feasible solutions with a sufficient level of accuracy with CPU times of less than 1 s.

© 2020 Elsevier Ltd. All rights reserved.

1. Introduction

For the year 2018, the total amount of electricity generation at global level was 26,700 TWh [1]. The major part of the increment of electricity consumption was covered by the generation corresponding to the new renewable and nuclear sources. Nevertheless, there was also an increase of the pollution level due fossil fuels. This increasing was of 2.4% in CO_2 emissions. In order to generate all the required electricity, is necessary the investment of large sums of money. In this context, electric companies are always seeking to improve the efficiency of power generation, transmission and distribution processes [2].

There are several strategies to improve the power system efficiency. One is to organize the power generation processes by implementing mathematical programming. It helps to decide the best combination of units for generating electricity to cover the forecast demand [3]. Another strategy is the implementation of systems that allow the storage of energy when the electricity demand is low. Then, the energy is returned to the system when the power demand is high [4]. The energy storage system can be classified into five groups: mechanical (Pumped Hydro-storage, Compressed Air, Flywheels), electric (superconductors, capacitors), thermal, electrochemical (batteries), and chemicals (fuel cells) [5].

Pumped Storage Hydropower Plants (PSHPs) are one of the most extended energy storage systems at worldwide level [6], with an installed power capacity of 153 GW [7]. The goal of this type of storage system is basically increasing the amount of energy in the form of water reserve [8]. During periods with low power demand (off-peak period), these systems pump water from a lower reservoir to an upper one. In contrast, when the electricity demand is increased (peak periods), PSHPs turbine water for producing electricity as a conventional hydropower plant. Countries that have the highest amounts of installed power capacity of this technology are China with capacity of 32 GW, Japan 28 GW, EUA 22 GW, and Spain 8 GW.

PSHPs have the advantage of presenting lower production costs, in comparison with the conventional generating units that are used during peak periods (as natural gas units or diesel units). As consequence of the PSHPs ability to pump water during off-peak periods, they take advantage of the variation in generation prices (the electricity prices are higher during the peak periods). In contrast to conventional hydropower plants, PSHPs do not depend

E-mail address: galvarez@santafe-conicet.gov.ar.

https://doi.org/10.1016/j.energy.2020.117797
0360-5442/© 2020 Elsevier Ltd. All rights reserved.

Nomenclature

Acronyms

PSHP	Pumped Storage Hydropower plant
MILP	Mixed integer linear programming
HUC	Hydro unit commitment
NLP	Nonlinear programming
MINLP	Mixed integer nonlinear programming
ISO	Independent system operator
RG-TP	Rio Grande this paper (curve of results with the new model)
LR-TP	Los Reyunos this paper (curve of results with the new model)
RG-9P	Rio Grande 9 points (curve of results with the nine point model)
LR-9P	Los Reyunos 9 points (curve of results with the nine point model)
RG-NL	Rio Grande nonlinear (curve of results with the nonlinear model)
LR-NL	Los Reyunos nonlinear (curve of results with the nonlinear model)

Indexes

s	index for each turbine or unit of the PSHP
t	index of time periods
z	index for head level
y	Index for generation segment

Constants

ρ_t^f	forecast hourly price
σ_s^{gen}	cost for generating 1 MW ($)
σ_s^{pu}	cost for consuming 1 MW ($)
S	total number of turbines
T	programming horizon
D_t	forecast demand (MW)
μ_s^{gen}	electric generator efficiency
μ_s^{turb}	hydraulic turbine efficiency
μ_s^{cp}	mechanical efficiency coupling between the turbine and the alternator
μ_s^{pu}	efficiency for the pumping mode
δ_{in}^{up}	inflow that correspond to the upper reservoir (m^3/s) or (Hm^3/h)
δ_{out}^{up}	outflow that correspond to the upper reservoir (m^3/s) or (Hm^3/h)
$\delta_{s,in}^{lo}$	inflow that correspond to the lower reservoir (m^3/s) or (Hm^3/h)
$\delta_{s,out}^{lo}$	outflow that correspond to the lower reservoir (m^3/s) or (Hm^3/h)
Δr_z^{min}	minimum volume difference for the head level$z$ (Hm^3)
Δr_z^{max}	maximum volume difference for the head level$z$ (Hm^3)
HD_z^{max}	maximum value of head level (m)
max_H	maximum head value for all levels (m)
HD_z^{min}	minimum value of head level (m)
$P_{y,z,s}^{gen}$	power generation at segments y, z for the unit s (MW)
$Dg_{y,z,s}$	discharge at segments y, z for the unit s (m^3/s) or (Hm^3/h)
$\overline{p_s^{gen}}$	maximum power output for each PSHP unit s
$\underline{p_s^{gen}}$	minimum power output for each PSHP unit s
$P_{z,s}^{pu}$	power consumption in pumping mode for the unit s and head$z$ (MW)
$Qp_{z,s}$	pumped water flow for the PSHP unit s and head$z$ (m^3/s) or (Hm^3/h)

Variables

$p_{s,t}^{gen}$	generated power (MW)
$p_{s,t}^{pu}$	consumed power (MW)
$Dg_{s,t}$	unit discharge variable (m^3/s) or (Hm^3/h)
$h_{s,t}$	hydraulic head (m)
$qp_{s,t}$	pumped water flow (m^3/s) or (Hm^3/h)
$\theta_{s,t}^{gen}$	binary variable that represents the generating mode status
$\theta_{s,t}^{pu}$	binary variable that represents the pumping mode status
ϕ_t^{gen}	binary to ensure that when a unit of the PSHP is working on pumping mode, the rest of units must not be in generating mode
ϕ_t^{pu}	binary to ensure that when a unit of the PSHP is working on generating mode, the rest of units must not be in pumping mode
r_t^{up}	upper reservoir water volume (Hm^3)
$r_{s,t}^{lo}$	lower reservoir water volume (Hm^3)
$wt_{y,z,s,t}^{gen}$	weight variable for generating mode [0,1]
$\tau_{z,s,t}$	binary variable for the for the head level matching
$wt_{z,s,t}^{pu}$	weight variable for pumping mode [0,1]

greatly on the river flows for increasing the volume of the upper reservoir. Additionally, PSHPs benefit from seasonal events due to the availability of pumping water from other reservoirs. As for the power system, PSHPs can respond quickly to several changes of power demands and they also participate in the control of grid frequency. Due to the aforementioned characteristics, these plants are preferred to cover peak demands [6].

Optimization techniques based on mathematical models that represent these PSHPs have greatly improved in recent years [9]. Hydro Unit Commitment Problem (HUC) involves finding the best possible combination to operate a conventional hydropower plant [10]. The problem which determines the operation of a PSHP is a special case of the HUC problem. In this field, a coordination framework to optimize a system integrated by PSHPs, irrigation facilities, and wind generators is developed in Ref. [11]. In Ref. [12], a nonlinear model (NLP) is presented for solving the HUC problem with two PSHPs from Iran, taking into account constraints of reservoir volumes and the diameter of the water transmission installations. The main drawback of NLP and Mixed Integer Nonlinear Programming (MINLP) models, which are implemented for representing PSHPs, is the elevated computational requirement to obtain solutions with a sufficient level of accuracy. For this reason, novel Mixed Integer Linear Programming (MILP) models have been developed for representing PSHPs during the last years. They allow to obtain the advantages of linear models, which are lower CPU times, global optimally, and the flexibility to add constraints [13]. Consequently, there are approaches, as in Ref. [14], that presents a linearization technique for the PSHP operating curves.

Unfortunately, the approach does not consider the effects of hydraulic head changes in the pumping mode. Hydraulic head is a measure of elevation from a water static column by considering an arbitrary point. In Ref. [15], this effect is considered as constant. In contrast [16], presents an MILP model for the operation of PSHPs, by using a nine-breakpoint method, which reduces the peak-valley difference of the residual load with head change effects. Another nine-breakpoint method is included in Ref. [17] to linearize the operation curves, but it is developed for conventional hydropower plants. A dynamic programming method is applied to solve multiple plants by considering head effects in Ref. [18]. However, this method is not efficient for the short-term scheduling due to dimensionality problems (as stated in Ref. [19]). In Ref. [20], a model that addresses a natural gas-electricity−hydraulic system is considered with a nine-point method. The main contributions and differences between the aforementioned works and the present paper are summarized in Table 1.

Argentine Republic is a country with a population of more than 40 million people and an extension of 2.78 million km^2. In order to provide electricity to the entire territory, a total power capacity of 38,609 MW is installed [21]. The participations of each generation technology in the energy matrix are described as follows (based on [21]). For thermal generation: steam turbine 11.5%, natural gas turbine 18%, combine cycle 29%, diesel 4.7%, and nuclear 4.5%. Additionally, the renewable sources are hydro 25.4%, pumped storage 2.6%, photovoltaic 0.5%, wind 2.1%, biogas 0.1% and other renewables 1.6%. The pumped storage technology has an installed capacity close to half of the nuclear power capacity (975 MW and 1755 MW, respectively). The pumped storage system of Argentine Republic is composed by two PSHPs: Los Reyunos that has two reversible turbines with 225 MW of installed capacity and Rio Grande with four turbines and 750 MW of capacity.

In view of the above, the main contribution of this paper is the introduction of a novel MILP model that deals with the operation of PSHPs (for both operating modes). The model considers several aspects that help to obtain more realistic solutions. It supports an elevated number of breakpoints. This constitutes the main difference when this model is compared against other models, which only can handle a reduced number of breakpoints. The implementation of a larger number of breakpoints enhances the quality of the solution. In addition, all constraints are considered simultaneously. This characteristic differentiates this model from other ones, as the decomposition methods. In addition, several constraints are also considered as water reservoir volumes, thresholds of operation, operating mode exclusivity, among others. The new model is applied to a real case formed by two PSHPs from Argentine Republic: Los Reyunos and Rio Grande. The daily programming of the two plants will be considered with real data provided by their owners (GENCOs) and the operator (ISO) [22]. This work is developed taking into account the linking between the grid ISO [23] and GENCOs.

The rest of this paper is organized as follows. Section 2 introduces the formulation of the PHSP operation, and develops the linearization technique to approximate the nonlinearities of operating curves. The numerical test based on the real case of the two PSHPs from Argentine Republic is presented and described in Section 3. Section 4 presents the analysis of results and compares the proposed model with similar ones. The conclusions of the study are drawn in Section 5.

2. Model for solving the power plant operations

This section presents and describes the original nonlinear model for the operation of PSHPs. After, it introduces the linearization techniques for obtaining a MILP model.

2.1. Operation constraints

The basic scheme of a PSHP can be observed in Fig. 1. The system is composed of an upper water reservoir and a lower reservoir. The difference between the water elevation from upper reservoir and the water elevation from lower reservoir is known as *hydraulic head* or, simply, *head*. Moreover, PSHPs have an internal system of penstocks with a reversible turbine which is connected to a generator. The plant provides electricity to a near power substation where the electricity is suited and transmitted to the grid (through transmission towers). The basic working of a PSHP is pumping water during periods when the electricity demand is low, usually at night. By contrast, when the electricity demand is increased and the generation prices are higher, PSHP turbines water for generating electricity. All water reservoirs depend on the water flows which are turbined or pumped by the PSHP, in addition to the river inflows and outflows.

Based on [24], the aim of the model is maximizing revenue (RG) of one PSHP by reducing the associate production cost for a programming horizon of 24 h. The objective function is presented in (1).

$$\max RG = \sum_{s=1}^{S}\sum_{t=1}^{T}\left[\rho_t^f\left(p_{s,t}^{gen} - p_{s,t}^{pu}\right) - p_{s,t}^{gen}\sigma_s^{gen} - p_{s,t}^{pu}\sigma_s^{pu}\right] \quad (1)$$

The model considers S turbines for a PSHP and the programming horizon is T. In addition, s is the index for each turbine or unit of the PSHP, t is the index of time periods, $p_{s,t}^{gen}$ is the generated power, $p_{s,t}^{pu}$

Table 1
Main contributions and differences of several approaches.

Approach	Main Contributions	Main Differences
[11]	Coordination framework to optimize the joint operation of pumped-storage unit, irrigation system and intermittent wind power generation	It is applied to a micro grid, not to a large scale system
[12]	NLP model for operating PSHP along with a comparison by using four criteria	NLP model can require an elevated computational effort, especially in large scale systems
[14]	A Linear model that address PSHP operation with the lowest computational effort along transmission constraints	It does not consider the hydraulic head effects for the pumping mode
[15]	A methodology that integrates predator-prey optimization (PPO) and Powell's search method	Hydraulic head is considered as constant
[16]	A MILP model to minimize the peak-valley difference of the residual load series of each power grid.	A nine-breakpoint method with nine triangles is applied to linearize
[17]	A MILP model for operating hydro generation, which requires fewer auxiliary variables	A nine-breakpoint method. The model only considers conventional hydropower plants. Without the capacity of pumping
[18]	Nonlinear model to address head effects of hydro systems	Inefficiency for short-term scheduling due to the dimensionality factor
[20]	A MILP model for solving a natural gas-electric-hydro system	A nine-breakpoint method with nine triangles is applied to linearize

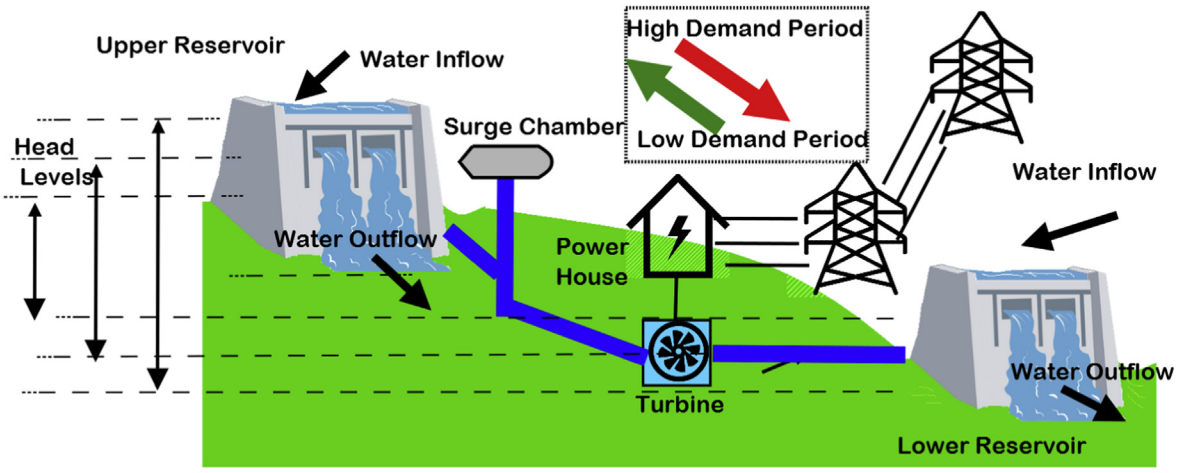

Fig. 1. Basic scheme of PHSP operation.

is the consumed power, ρ_t^f is the forecasted hourly price for each time t, σ_s^{gen} and σ_s^{pu} are the costs for unit capacity. In the considered case, both costs will be assumed as negligible.

When the problem includes system constraints, the first one is satisfying the power demand, which is represented in (2). Where D_t is the forecast power demand at time t that is reported by the ISO in a deregulated electricity market [25]. It is important to mention that D_t refers to the generation that the ISO expect from the PSHP.

$$\sum_{s=1}^{S} p_{s,t}^{gen} \geq D_t \quad , \quad t = 1, \ldots, T \tag{2}$$

Based on [26], the generated power by a PSHP is calculated in (3). Where $Dg_{s,t}$ is the unit discharge variable, which represents the rate of water flow through the water control facilities. The variable is related to the flow rate of each individual unit. As a consequence, $Dg_{s,t}$ is the amount of cubic meters of water that pass through the turbine s at time t. In addition, $h_{s,t}$ is the head variable, μ_s^{gen} is the electric generator efficiency (from 0.92 to 0.97), μ_s^{turb} is the hydraulic turbine efficiency (from 0.75 to 0.94), and μ_s^{cp} is the mechanical efficiency coupling between the turbine and the alternator (from 0.95 to 0.99).

$$p_{s,t}^{gen} = 9800\, Dg_{s,t} h_{s,t} \mu_s^{gen} \mu_s^{turb} \mu_s^{cp} \Big/ \left(1 * 10^6\right), \ldots\ldots\ S = 1, \ldots, S; t = 1, \ldots, T \tag{3}$$

Based on [27], the power consumed by the PSHP for pumping water is calculated in (4). This equation depends on the variables of pumped water $qp_{s,t}$ and head$h_{s,t}$. Accordingly, there is a product between the two continue variables, as in case of power generation constraint (3). Consequently, both nonlinear constraints are hard to solve due to the elevated computational requirement.

$$p_{s,t}^{pu} = \frac{9800 qp_{s,t} h_{s,t}}{\mu_s^{pu} 1 * 10^6} \quad s = 1, \ldots, S; t = 1, \ldots, T \tag{4}$$

In order to avoid mechanical problems for the PSHPs, an exclusivity constraint of operation mode is needed. As a result, when one or more units of the plant are working in generating or pumping mode, the rest of the units must be working in the same operation mode or in off status. For this purpose, two binary variables are introduced for representing the generating mode ($\theta_{s,t}^{gen}$) and the pumping mode ($\theta_{s,t}^{pu}$). Mode exclusivity constraints are developed in (5-10). Constraint (5) imposes that only one of the two binary variables is equal to 1 when the PSHP is generating, pumping, or 0 otherwise.

$$\theta_{s,t}^{gen} + \theta_{s,t}^{pu} \leq 1 \ldots\ldots s = 1, \ldots, S; t = 1, \ldots, T \tag{5}$$

The binary variable ϕ_t^{gen} is set up so that if one unit of the PSHP is in generating mode, the rest of units cannot be in pumping mode. In fact, $\phi_t^{gen} = 1$ when at least one unit is in generating status. This mode exclusivity is modeled in (6–7). Thus, if $\theta_{s,t}^{pu} = 1$ for the units, all $\theta_{s,t}^{gen} = 0$. In another case, if $\theta_{s,t}^{pu} = 0$ for the units, all $\theta_{s,t}^{gen} = 0$ or 1. This exclusivity of operating mode is modeled in (6) as follows.

$$\sum_{s=1}^{S} \theta_{s,t}^{gen} \leq S\, \phi_t^{gen}, \quad t = 1, \ldots, T \tag{6}$$

A similar reasoning is adopted in constraint (7). In this case, the binary variable ϕ_t^{pu} is implemented to avoid the overlapping of operating modes.

$$\sum_{s=1}^{S} \theta_{s,t}^{pu} \leq S\, \phi_t^{pu}, \quad t = 1, \ldots, T \tag{7}$$

Constraint (8) establishes that all units of the PSHP can be included within the three stages for each time period: at least one unit is in pumping mode, generating mode, or all units are in off status.

$$\phi_t^{pu} + \phi_t^{gen} \leq 1, \quad t = 1, \ldots, T \tag{8}$$

Constraints (9) and (10) determinate the water volumes of the upper and lower reservoirs. These constraints include the variables related to pumped and turbined water flows, along with the constants that represent the river inflows or outflows which are connected to the reservoirs. The model considers a PSHP with one upper reservoir and several lower reservoirs. In this context, the model includes all possible configurations of PSHPs.

$$r_t^{up} = r_{t-1}^{up} + \delta_{in}^{up} + \delta_{out}^{up} - \sum_{s=1}^{S} Dg_{s,t} + \sum_{s=1}^{S} qp_{s,t}, \qquad t = 1, \ldots, T \tag{9}$$

$$r_{s,t}^{lo} = r_{t-1}^{lo} + \delta_{s,in}^{lo} + \delta_{s,out}^{lo} + Dg_{s,t} - qp_{s,t}, \ldots\ldots\ s = 1, \ldots, S; t = 1, \ldots, T \tag{10}$$

The proposed model considers that each unit s can be connected to different reservoirs. If all units share the same reservoirs and they are installed at the same height, values of head variable can be set as equals for all units of each PSHP and each$t$ (in order to reduce the computational effort). Besides, river inflows and outflows are considered as constants for the daily scheduling [28].

Constraint (11) ensures that the amount of water volume in the upper reservoir, at the end of the programming horizon, must be greater than or equal to the water volume at the beginning. This constraint constitutes an energy reserve.

$$r_{t=T}^{up} > r_{t=1}^{up} \tag{11}$$

2.2. Mixed integer linear programming model

This subsection presents the linearization techniques that are implemented for solving the PHSP operations with the novel MILP model.

2.2.1. Generating mode

There are some papers, as the aforementioned in the Introduction, which have linearized the nonlinear PSHP operating curves presented in (3) by considering the head variation effects. However, these papers admit up to nine breakpoints which are divided into three head levels and three generation segments. These models solve the problem throught the implementation of a nine triangles sub-region method. By contrast, the model presented in this paper admits an increased number of breakpoints with more head levels and generation segments. This means an enhancing of the accuracy level of the obtained solutions. Graphical representation of the relation between the water discharge and power generation for PSHPs is drawn in Fig. 2. The figure includes real data belonging to the unit 1 of PSHP Los Reyunos and the unit 1 of PSHP Rio Grande, based on [29].

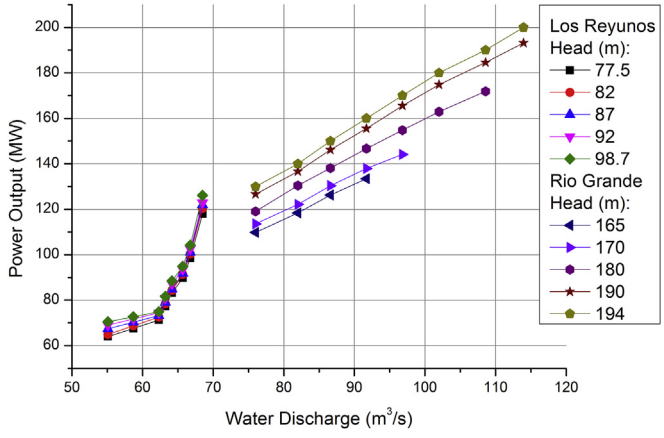

Fig. 2. Discharge-generation curves belonging to real cases of PSHPs Los Reyunos and Rio Grande.

Graph included in Fig. 2 represents performance curves for five levels of hydraulic head, which correspond to 194 m, 190 m, 180 m, 170 m, and 195 m for Rio Grande. In the case of Los Reyunos, head levels are 98.7 m, 92 m, 87 m, 82 m, and 77.5 m. Regarding the generation mode, eight segments are considered which are 130 MW, 140 MW, 150 MW, 160 MW, 170 MW, 180 MW, 190 MW, and 200 MW for Rio Grande. Segments for Los Reyunos are 64 MW, 67.6 MW, 71.2 MW, 77.2 MW, 83.1 MW, and 89.7 MW.

In order to linearize the PSHP performance curves, several constraints will be introduced. Constraint (12) implies that the binary variable $\theta_{s,t}^{gen}$ is equal to the sum of all generating mode weight variables $wt_{y,z,s,t}^{gen}$ [0,1]. Where y is the index for generation segment, z is the index for head level, Y is the total number of generation segments, and Z is the total number of head levels. The sum of the weight variables is equal to the binary variable$\theta_{s,t}^{gen}$. When the unit is generating the value of the sum is equal to 1.

$$\sum_{y=1}^{Y}\sum_{z=1}^{Z} wt_{y,z,s,t}^{gen} = \theta_{s,t}^{gen}, \qquad s = 1, \ldots, S; t = 1, \ldots, T \tag{12}$$

Constraint (13) relates the reservoir volume differences with the binary variable $\tau_{z,s,t}$. This variable is equal to 1 when the difference between reservoir volumes matches with the corresponding head level and 0 otherwise. Δr_z^{min} and Δr_z^{max} are constants that represent the minimum and maximum volume difference for the head level z.

$$\sum_{z=1}^{Z} \tau_{z,s,t}\Delta r_z^{min} \le r_t^{up} - r_{s,t}^{lo} \le \sum_{z=1}^{Z} \tau_{z,s,t}\Delta r_z^{max}, \quad s = 1, \ldots, S; t = 1, \ldots, T \tag{13}$$

Constraints (14–15) calculate the value of the head variable $h_{s,t}$ for each unit s by considering the weight variable $wt_{y,z,s,t}^{gen}$. Where HD_z^{max} and $HD_z^{min}$are constants that correspond to the maximum and minimum value of head level. In addition, max_H is the maximum head value for all levels.

$$h_{s,t} \le \sum_{y=1}^{Y}\sum_{z=1}^{Z} wt_{y,z,s,t}^{gen} HD_z^{max} + \max\_H\left(1 - \theta_{s,t}^{gen}\right), \quad s = 1, \ldots, S; t = 1, \ldots, T \tag{14}$$

$$h_{s,t} \ge \sum_{y=1}^{Y}\sum_{z=1}^{Z} wt_{y,z,s,t}^{gen} HD_z^{min}, \qquad s = 1, \ldots, S; t = 1, \ldots, T \tag{15}$$

The values of the power output ($p_{s,t}^{gen}$) and water discharge ($Dg_{s,t}$) variables are defined by constraints (16–17). Where $P_{y,z,s}^{gen}$ and $Dg_{y,z,s}$ are constants related to the power generation and water discharge of the unit at segments y, z.

$$p_{s,t}^{gen} = \sum_{y=1}^{Y}\sum_{z=1}^{Z} wt_{y,z,s,t}^{gen} P_{y,z,s}^{gen}, \qquad s = 1, \ldots, S; t = 1, \ldots, T \tag{16}$$

$$Dg_{s,t} = \sum_{y=1}^{Y}\sum_{z=1}^{Z} wt_{y,z,s,t}^{gen} Dg_{y,z,s}, \qquad s = 1, \ldots, S; t = 1, \ldots, T \tag{17}$$

Units of the PSHP have maximum and minimum operating limits due to security and technical reasons, this is modeled in (18). Where $\overline{p_s^{gen}}$ and $\underline{p_s^{gen}}$ are the power output limits for each PSHP units.

$$\overline{p_s^{gen}}\,\theta_{s,t}^{gen} \le p_{s,t}^{gen} \le \theta_{s,t}^{gen}\,\underline{p_s^{gen}}, \quad s=1,\ \ldots,S; t=1,\ \ldots,T \tag{18}$$

In order to enhance the understanding of the method of this section, it is important to mention that constraint (12) sets the weighting sum of all breakpoints. In fact, if a unit is in generating mode, the weighting sum is equal to 1 and 0 otherwise. Besides, constraints (14–15) calculate the interpolation value for the head variable. If the unit is generating, the interpolated value will be equal to the weighted head sum for each breakpoint. Finally, (16–17) calculate the weighted sum of the power output and water discharge, respectively. These five constraints depend on the weighted variable$wt_{y,z,s,t}^{gen}$. It establishes the operation point for the unit and it maintains the variables$p_{s,t}^{gen}$,$h_{s,t}$ and $Dg_{s,t}$ in concordance. The dependencies and dynamism between these variables and the weighted variables have been widely discussed in Ref. [17]. Fig. 3 illustrates the breakpoint implementation and the differences between traditional models and the new model. Fig. 3 A) represents the traditional method to determine the operating point. This method is based on the use of nine breakpoints that correspond to the real generation-discharge curves of the PSHP. Each breakpoint is obtained due to the intersections between the three head levels and the three generation segments. The operating point is determined by selecting one of the nine triangles (which are marked in the figure) by implementing auxiliary variables. The sum of the weight variables will be influence by the head levels and the generation segments. The major disadvantage of the method is that it can only handle nine breakpoints. By contrast, Fig. 3 B) shows the proposed method which supports a higher number of head levels, generation segments and, in consequence, a greater amount of breakpoints. The method can determine the correct portion of the operating zone. As more real breakpoints contribute to represent the generation-discharge curves, more realistic solutions are obtained.

2.2.2. Pumping mode

Similar reasoning of the previous subsection applies to the pumping mode. Constraint (19) implies that the sum of the weight variables of pumping mode $wt_{y,z,s,t}^{pu}$ must be equal to the binary variable for pumping status $\theta_{s,t}^{pu}$.

$$\sum_{z=1}^{Z} wt_{z,s,t}^{pu} = \theta_{s,t}^{pu}, \qquad s=1,\ \ldots,S; t=1,\ \ldots,T \tag{19}$$

Values belonging to the power consumption variable $p_{s,t}^{pu}$ and the pumped water variable $qp_{s,t}$ are calculated through constraints (20–21). Where $P_{z,s}^{pu}$ is the constant for the power consumption, and $Qp_{z,s}$ is the constant related to the pumped water flow (for the unit s along with the head level z).

$$p_{s,t}^{pu} = \sum_{z=1}^{Z} wt_{z,s,t}^{pu} P_{z,s}^{pu}, \qquad s=1,\ \ldots,S; t=1,\ \ldots,T \tag{20}$$

$$qp_{s,t} = \sum_{z=1}^{Z} wt_{z,s,t}^{pu} Qp_{z,s}, \qquad s=1,\ \ldots,S; t=1,\ \ldots,T \tag{21}$$

The binary variable $\tau_{z,s,t}$is introduced to avoid discrepancies of operating points, especially when the PSHP goes from the generating mode to the pumping mode, or vice versa. More specifically, the variable is equal to 1 when the operating point matches with the head level z and 0 otherwise. In consequence, $\tau_{z,s,t}$ will be implemented in the next five constraints to establish the interdependencies among discharges, pumping flows, and the reservoir conditions. To determine the correct value of$\tau_{z,s,t}$, constraint (22) implies that the variable must be active in a single head level. This constraint relates the water reservoir differences with the values of the rest of variables, which depend on the head level.

$$\sum_{z=1}^{Z} \tau_{z,s,t} = 1; \quad s=1,\ \ldots,S; t=1,\ \ldots,T; z=1,\ldots,Z \tag{22}$$

Variable $\tau_{z,s,t}$ is related to the weight variables for both operating modes, $wt_{y,z,s,t}^{gen}$ and$wt_{z,s,t}^{pu}$, in constraints (23–24).

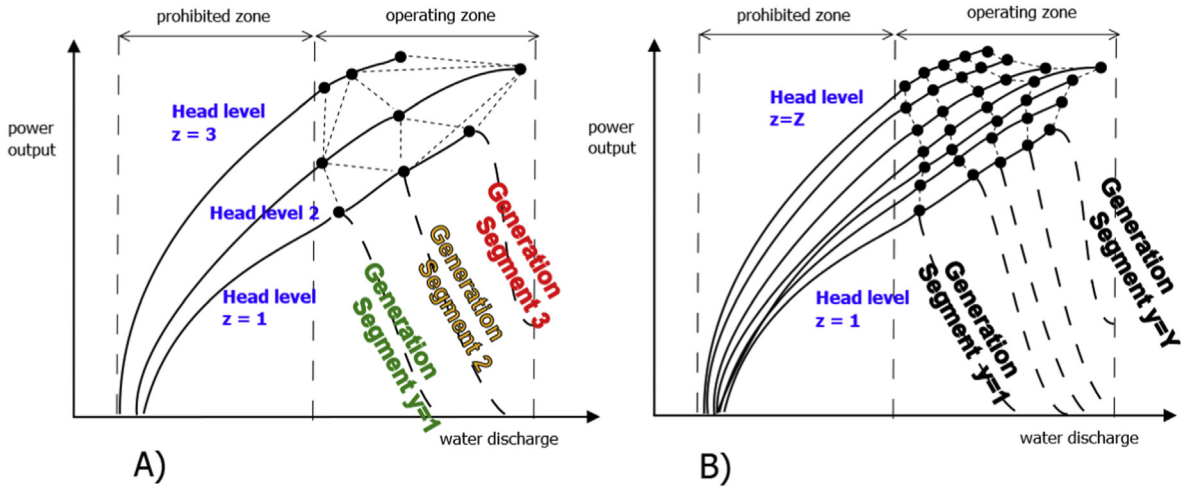

Fig. 3. Comparison between A) traditional nine-breakpoint models and B) the novel model.

$$\sum_{y=1}^{Y} wt_{y,z,s,t}^{gen} \le \tau_{z,s,t}, \qquad s = 1, \ldots, S; t = 1, \ldots, T; z = 1, \ldots, Z \tag{23}$$

$$wt_{z,s,t}^{pu} \le \tau_{z,s,t}, \qquad s = 1, \ldots, S; t = 1, \ldots, T; z = 1, \ldots, Z \tag{24}$$

Constraints (25–26) relate the binary variable $\tau_{z,s,t}$ with the determination of the head value. Where $M$is a sufficiently large positive number.

$$h_{s,t} - M(1 - \tau_{z,t}) \le \tau_{z,s,t} HD_z^{max}, \qquad s = 1, \ldots, S; t = 1, \ldots, T; z = 1, \ldots, Z \tag{25}$$

$$h_{s,t} + M(1 - \tau_{z,t}) \ge \tau_{z,s,t} HD_z^{min}, \qquad s = 1, \ldots, S; t = 1, \ldots, T; z = 1, \ldots, Z \tag{26}$$

Fig. 4 illustrates the flowchart of the proposed methodology along with an identification of steps. It is convenient to mention that the model considers simultaneously all constraints. The method is divided into steps in order to enhance the understanding of the reader. The inputs are data relating to hourly electricity prices, operating costs, and the forecast demand. The model determines when is more convenient to generate or consume electricity, in order to maximize the benefits of the PSHP GENCOs. To obtain the optimal decision about the operation of the plants, the model needs an efficient exploration of the generation-discharge curves, consumption-pumping curves, and the reservoir dynamics. The operating curves are nonlinear and solve them require an elevated computational effort. Even it could be impossible to obtain feasible solutions within a reasonable time (many authors consider this limit as 3600 s). For this reason, the model solves the determination of the operating point through the linearization of curves. However, linearization of operating curve can lead to obtain solutions that are far from the reality. The most majority of linearization models consider up to nine breakpoints. In connection with this issue, the proposed model considers a better representation of the real curves based on the inclusion of more breakpoints. The novel formulation allows the utilization of an elevated number of breakpoints to enhance the obtained solutions. Main differences between the traditional models and the novel proposal were shown in the Fig. 3. The more implemented breakpoints, the better the quality of the solution. These improvements of the curve linearization will be proved and discussed in the next sections.

3. Case study

The proposed MILP model is applied to a real system that is the Pumped Storage System of Argentine Republic. The system is formed by two PSHPs. First one is Los Reyunos Plant, which is located in Mendoza province. It has two units with a total installed power capacity of 225 MW and its yearly generation is about 247 GWh. The upper reservoir is called Los Reyunos and the lower reservoir is El Tigre.

The second plant is called Rio Grande, which is the largest PSHP in Latin America. It is located in Cordoba province and its yearly generation is about 970 GWh. The upper reservoir of the plant is called Cerro Pelado and the lower one is Arroyo Corto. The tributary of river only offers a 15% of the required water volume for generating power. As a consequence, 85% of the required water volume is pumped from the lower reservoir. Power capacity of Rio Grande is 750 MW along with four Francis reversible turbines. The basic scheme of the two PSHPs is shown in Fig. 5. Plants are marked in the geographical space of South America.

Data relating to generation and discharge for the two PHSPs are given in Table 2. In addition, Table 3 presents information concerning reservoirs. Both tables were formulated based on [29–31]. The hourly forecast price for the 24 h of programming horizon is given in Table 4. In addition, Table 5 presents the hourly demand that each PSHP must cover according to the requirements of ISO CAMMESA, which is in charge of organizing the power generation of the whole country [32]. It is important to mention that the model of Section 2 represents the operation of a single PSHP. In the case of this test system, the total revenue is obtained from the sum of two objective functions and the respective constraints of each plant (one model is implemented for each PSHP). This is revealed in the model size description in the next section.

4. Analysis of results and comparisons

The CPU equipment used for solving the test system is an INTEL CORE i5 750 @ 2.67 GHz processor and 4 GB of RAM. The model was programmed using software GAMS and the linear solver CPLEX [33]. Adopted relative GAP is 0.05%. Note that the relative GAP is the difference between the best known solution and the value that bounds the best possible solution, divided by the best bound.

4.1. Results of the two plant operation

The MILP model is composed of 5331 equations, 8,065 single variables and 1344 binary variables. The model is solved by CPLEX within a CPU time of 0.9 s and the solution value is $ 169,688. Since all units of each PSHP are installed at the same height of the test case, the amount of head variables could be reduced (to one head variable for each PSHP). However, in order to keep the general purpose and application of the model, head variables are considered as in Section 2. It is also important to mention that the model optimizes both PSHPs simultaneously.

In Fig. 6 there are 2 bar graphs that show the power output profile for the two PSHPs (on the left side of the vertical axis) and the hourly price during 24 h of the programming horizon (on the right side of the vertical axis). Positive values of y-axis represent power generation. By contrast, negative values represent power consumption. The graph on the left belongs to Rio Grande and the graph on the right belongs to Los Reyunos. According to the obtained solution, Rio Grande is working at rated power during the first hour, it pumps water between hours 2 and 8 with a consumption of 4320 MWh, it is in off status between hours 9–17, it generates 3889 MWh during 18–23 h (interval with the highest hourly price), and it is in off status at the last hour. The plant generates 4649 MWh during the whole programming horizon and consumes 4320 MWh. There is a significant economic benefit, in spite of the power generation and consumption amounts are very similar. As a consequence, it can be noted that the model takes advantage of the price variations. Hourly prices are lower during the off-peak power demand periods and higher during the peak periods. As a result, Rio Grande gets a gross profit of $345,927 along with an operating cost of $245,957 and, consequently, a net profit of $ 99,970. It is important to mention that the generating-discharge curves for Rio Grande are similar to straight lines. In fact, they can be addressed though methods which consider these particularities (for example, as is treated in Ref. [34]). For the purposes of this paper, curves are linearized by using constraints of the section 2.1.

For Los Reyunos Plant, the hourly operation is given in the

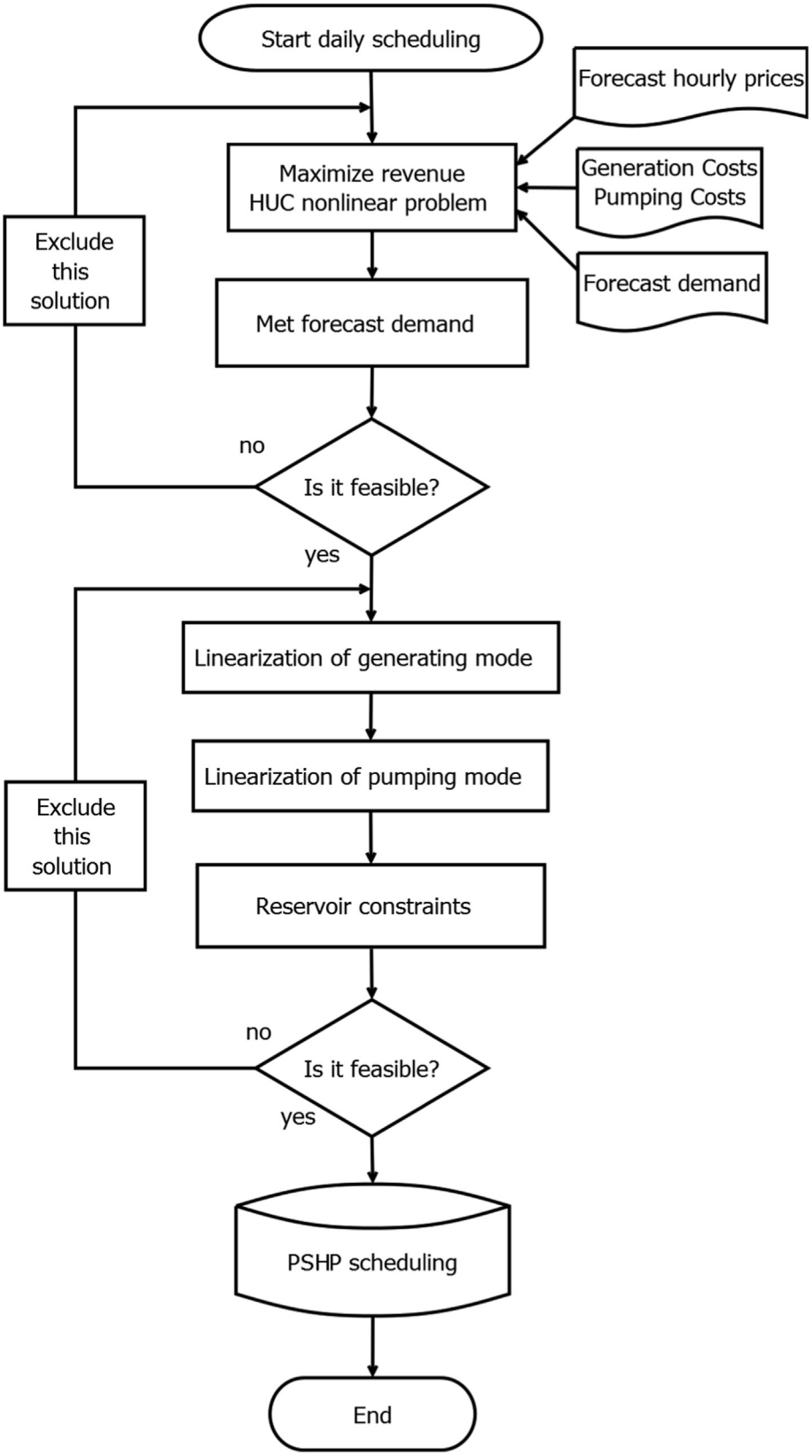

Fig. 4. Flowchart of the novel MILP model.

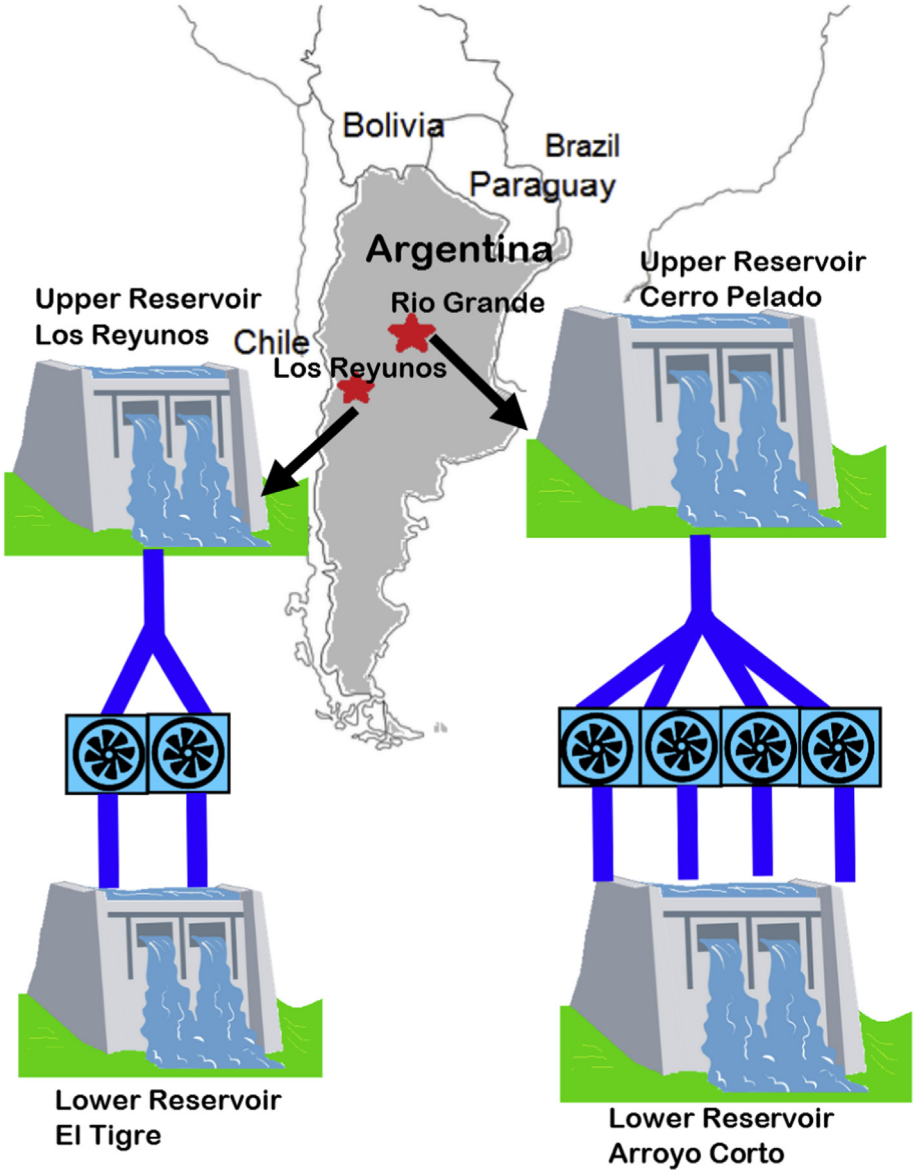

Fig. 5. Basic scheme of PHSPs Los Reyunos and Rio Grande.

following form: it generates 236 MWh for the first hour, 128 MWh for the hour 4, and 1234 MWh between hours 18–23. With regard to the power consumption for pumping water, Los Reyunos consumes 236 MWh between hours 2–3, 472 MWh between hours 5–6, and 118 MWh during hour 9. This PSHP generates 1598 MWh and consumes 826 MWh during the whole programming horizon. As a result of hourly prices, the plant has a gross profit of $115,836, an operating cost of $47,117, and thus a net profit of $69,719.

Regarding revenue prices, the forecast demand (expressed in Table 4) is required to the authorized GENCOs by the ISO and this requirement is mandatory. In this context, GENCOs sell their generation in the Argentinean Electricity Market. In this market, the generation that is used to cover the forecast demand is paid in the Seasonally Market according to the hourly forecast prices. Moreover, when the generation exceeds the forecast demand, it is sold in the Spot Market (where prices vary during each hour according the demand changes and unit availability). In this paper, prices of both markets are assumed as equivalent.

Fig. 7 shows two graphs that represent head level on the left vertical axis, and the volumes of upper and lower reservoirs on the right vertical axis. As in the previous figure, graph on the left side belongs to Rio Grande and graph on the right belongs to Los Reyunos. For Rio Grande Plant, the head value is 180 m for the hours 1, 23, and 24. During the rest of periods (hours 2–22), the head value is 190 m. As regards water reservoir volumes, it can be observed that there is an almost proportional relationship between the volumes of Cerro Pelado (upper reservoir) and Arroyo Corto (lower reservoir). The volume of Cerro Pelado increases its value from 201.3 Hm^3 to 209 Hm^3 during hours 1–10 due to the pumping operation. As a consequence of the pumped water flow, the volume of Arroyo Corto decreases its value from 14.36 Hm^3 to 7.41 Hm^3 in the same period. By contrast, the volume of Cerro Pelado decreases from 209.25 Hm^3 to 201.30 Hm^3 between hours 18 and 24, due to power generation. Lastly, the volume of Arroyo Corto increases from 7.71 Hm^3 to 16.30 Hm^3.

As regards Los Reyunos Plant, the head value is 86.9 m between

Table 2
Water discharge of the two PSHPs (m^3/s).

Los Reyunos - Unit 1					
Generation Segment (MW)	Head Levels (m)				
	Head 1 $z_1 = 77.5$	Head 2 $z_2 = 82$	Head 3 $z_3 = 87$	Head 4 $z_4 = 92$	Head 5 $z_5 = 98.7$
$y_1 = 64$	55.1	54.3	52.3	51.1	50
$y_2 = 67.62$	58.7	57.76	56.46	55.37	54.62
$y_3 = 71.24$	62.3	61.22	60.63	59.64	59.25
$y_4 = 77.19$	63.24	62.25	61.76	60.43	59.79
$y_5 = 83.14$	64.18	63.29	62.89	61.22	60.33
$y_6 = 89.79$	65.69	64.61	64.22	63.04	62.16
$y_7 = 98.50$	66.77	65.59	65.07	64.18	63.1
$y_8 = 81.18$	68.5	67.2	66.3	65.8	64.1
Rio Grande - Unit 1					
Generation Segment (MW)	Head Level (m)				
	Head 1 $z_1 = 165$	Head 2 $z_2 = 170$	Head 3 $z_3 = 180$	Head 4 $z_4 = 190$	Head 5 $z_5 = 194$
$y_1 = 130$	90	87	83	78	76
$Y_2 = 140$	97	94	88	84	82
$y_3 = 150$	102.87	99.61	94.06	88.87	86.6
$y_4 = 160$	109.94	106.33	100.01	94.33	91.69
$y_5 = 170$		114.17	106.31	99.43	96.8
$y_6 = 180$			112.68	105.03	101.98
$y_7 = 190$			120.03	111.75	108.56
$y_8 = 200$				117.98	113.94

Table 3
Data reservoirs of the two PSHPs.

Item	Los Reyunos		Rio Grande	
	Lower Reservoir El Tigre	Upper Reservoir Los Reyunos	Lower Reservoir Arroyo Corto	Upper Reservoir Cerro Pelado
Minimum volume (Hm^3)	0	58	0	0
Maximum volume (Hm^3)	8	271	34.5	565
Initial volume (Hm^3)	2.9	154.2	14.4	201
River Inflow (Hm^3/h)	0.1	0.1	0.1	0.1
River Outflow (Hm^3/h)	0.05	0.05	0	0
Min. volume difference Head level 1 (Hm^3)	0		−35	
Min. volume difference Head level 2 (Hm^3)	75		15	
Min. volume difference Head level 3 (Hm^3)	108		81	
Min. volume difference Head level 4 (Hm^3)	152		187	
Min. volume difference Head level 5 (Hm^3)	203		348	
Max. volume difference Head level 1 (Hm^3)	75		15	
Max. volume difference Head level 2 (Hm^3)	108		81	
Max. volume difference Head level 3 (Hm^3)	152		187	
Max. volume difference Head level 4 (Hm^3)	203		348	
Max. volume difference Head level 5 (Hm^3)	270		557	

Table 4
Hourly forecast price.

Hour	$\rho_t^f\left(\frac{\$}{MW}\right)$	Hour	$\rho_t^f\left(\frac{\$}{MW}\right)$	Hour	$\rho_t^f\left(\frac{\$}{MW}\right)$	Hour	$\rho_t^f\left(\frac{\$}{MW}\right)$
1	59.57	7	57.51	13	69.01	19	72.71
2	54.23	8	60.80	14	68.61	20	78.26
3	56.69	9	62.03	15	66.14	21	78.87
4	57.10	10	65.73	16	65.93	22	78.67
5	56.49	11	66.14	17	66.76	23	78.07
6	56.69	12	66.55	18	72.71	24	76.00

Table 5
Hourly forecast demand (MW).

Hour	Rio Grande	Los Reyunos	Hour	Rio Grande	Los Reyunos
1–17	0	0	21	725.25	217.58
18	562.50	168.75	22	637.5	191.25
19	667.50	200.25	23	525	157.50
20	727.50	218.25	24	0	0

hours 1 to 5, 91.9 m during hours 6–18, and 86.9 m during hours 19–24. The volume of the upper reservoir (Los Reyunos Reservoir) is increased in a fluctuant manner from 154.16 Hm^3 to 156.32 Hm^3. Consequently, the volume of the lower reservoir (El Tigre) is increased from 2.96 Hm^3 to 3.34 Hm^3 between hours 1 and 17. It should be noted that the volume of El Tigre is also increased, even with the water discharge for power generation. This results from the fact that the river tributary is a significant contribution to the volume reservoir. Subsequently, Los Reyunos Reservoir decreases its volume from 156 Hm^3 to 154.16 Hm^3 due to power generation (between hours 18 and 24), and the volume of El Tigre increases from 3.83 Hm^3 to 6.14 Hm^3.

4.2. Model comparison

It is important to mention that when it came to solving the test system by applying the original nonlinear model (1-11), it was not possible to obtain feasible solutions using nonlinear solvers BARON, DICOPT, and SBB [35]. In these cases, the time limit was 3600 s. To study the accuracy of the new model, a comparison among three models can be observed in Fig. 8. First one is the model proposed in

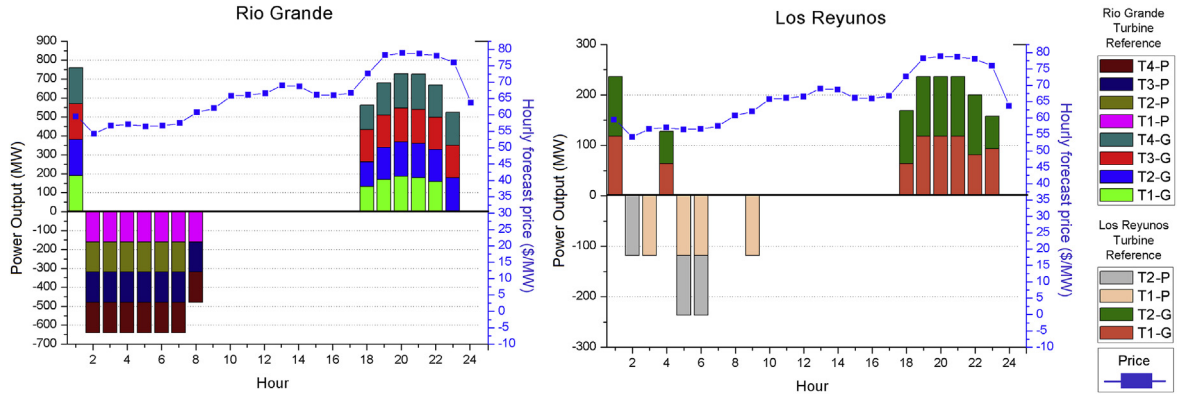

Fig. 6. Generation and consumption profile for PSHPs Los Reyunos and Rio Grande.

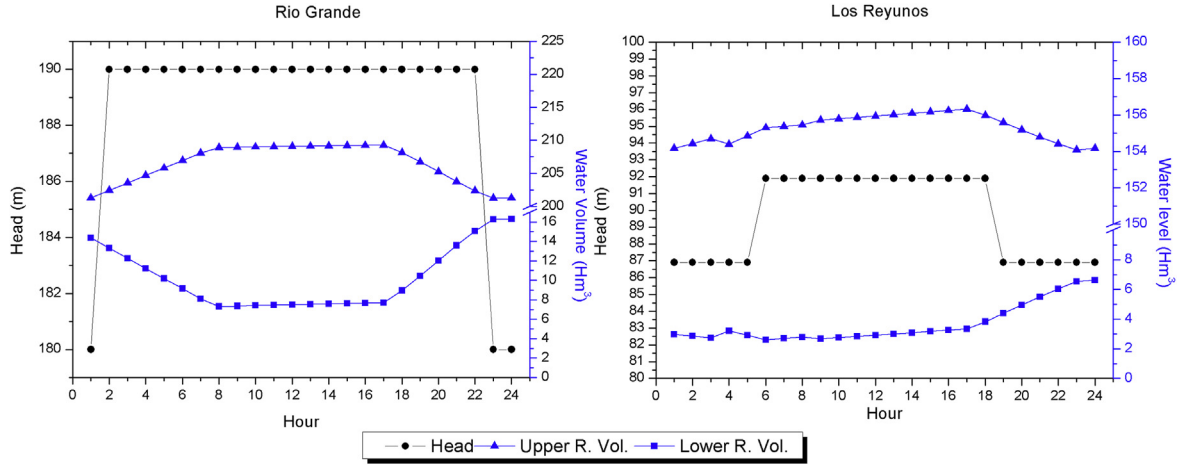

Fig. 7. Volumes of reservoirs and head level for PSHPs Los Reyunos and Rio Grande.

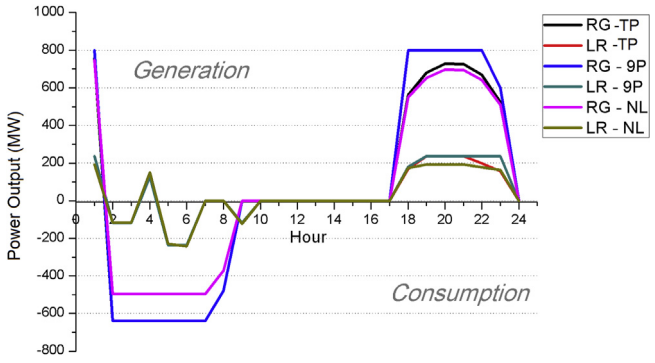

Fig. 8. Comparison among three models for power consumption and generation.

this paper, called *TP* model, whose curves of results are labeled as *RG-TP* for Rio Grande and *LR-TP* for Los Reyunos. Second one is the classic linear model of nine breakpoints, called *9P* model, whose curves of results are labeled as *RG-9P* for Rio Grande and *LR-9P* for Los Reyunos. In order to obtain a *9P* model for solving the test system, only three head levels and three generation segments of Table 2 are taken into account. The considered head levels are z_1, z_3, z_4, and the considered generation segments are y_1, y_4, y_8. Three auxiliary variables also are needed to obtain the *9P* model. These variables are implemented to locate the operating point within one of the nine triangle sub-regions. The third model is the nonlinear model and it is obtained by implementing nonlinear constraints (3–4). However, values for head and water flow variables are taken from the solution of the *TP* model to calculate the power output. This is because, as stated at the beginning of the section, it is impossible to obtain solutions by using the original nonlinear model without initial values. Curves of results that belong to the nonlinear model, called *NL* model, are labeled as *RG-NL* for Rio Grande and *LR-NL* for Los Reyunos.

In the figure, positive values of curves correspond to the power generation ($p_{s,t}^{gen}$) and negative values correspond to the power consumption ($p_{s,t}^{pu}$). The total generation or consumption of all units is considered for each curve. Regarding power generation in the first hour, the *RG-TP* curve value is 760 MWh, *RG-9P* is 800 MWh, *RG-NL* is 745.87 MWh, *LR-TP* and *LR-9P* are 236 MWh, and *LR-NL* is 132.4 MWh. During hour 12 LR-*TP* is 128 MWh, *LR-9P* is 128 MWh, and *LR-NL* 151.3 MWh. Between hours 18 and 23 the averages of curves are 648.14 MWh, 205.63 MWh, 624.4 MWh, 226.8 MWh, 624.4 MWh, and 182 MWh for the six curves in the order that they have been referred in the figure, respectively. On the other hand, the values of power consumption for three curves (*LR-TP, LR-9P, LR-NL*) during hour 4 are 128, 128, and 151.3 MWh. Finally, the averages during the rest of pumping periods for the six curves are 617, 165.2, 617.1, 165.2, 478, and 165 MWh, respectively. The NL model generates a total amount of 5928 MWh and consumes 4171 MWh. This means that there are differences of 5.09% for *TP* model and

5.47% for *9P* model, when the total generated power is considered. In case of power consumption, the difference between *NL* and both linear models (*TP* and *9P*) is 18.93%.

Visual analysis of the figure suggests that, when the power consumption periods are considered, there are not differences between curves *RG-TP* and *RG-9P* or between curves *LR-TP* and *LR-9P*. In addition, when the power generation during hour 1 is considered, a slight difference can be appreciated between the values of curves *RG-TP* and *RG-9P*, because *RG-TP* curve value is closer to the value of the *RG-NL*. The main differences of curves are observed between hours 17 and 29. When the curves of results for models *TP* and *9P* are compared during these periods, it can be observed that the values for *RG-TP* and *LR-TP* curves are closer to the values of *RG-NL* and *LR-NL*.

Another analysis related to the study of the accuracy level is the implementation of the factor∂_t, which is calculated in (27). It is obtained from the absolute value of the difference between the power generation (or consumption) curve values of each linear model (*TP* and *9P*) and the power generation (or consumption) curve value for the nonlinear model (RG-NL and LR-NL), divided by the absolute value of the point that belongs to the nonlinear model curve. The lower the value of∂_t, the better the accuracy level of the linear model.

$$\partial_t = \frac{|linear\ value_t - non\ linear\ value_t|}{|non\ linear\ value_t|} * 100; \qquad t = 1, \ldots, T \tag{27}$$

Table 6 shows the values for ∂_t that are obtained from the comparison between the two linear models, *TP* and *9P*, for the two PSHPs (*RG* and *LR*). It can be observed that ∂_t values of *TP* model are lower than the values of *9P* model during hour 1, and they are also lower between hours 18 and 24. There are not values of ∂_t during the rest of the programming horizon because PSHPs are in off status, or the values of ∂_t for both linear and nonlinear models are equal. Values of ∂_t for the *9P* model are at no time lower than the values of *TP* model.

Finally, a third comparison between the two linear models can be formulated. Besides the visual analysis through curve graphs and the study of ∂_t values, another comparison of both models is presented. It considers the total amounts of water discharge and pumped water flow during the programming horizon. The analysis of discharge and pumped water flow is presented in Fig. 9. Curves of *TP* model for both PSHPs are labeled as *RG-TP* and *LR-TP*, and curves of 9P model are labeled as *RG-9P* and *LR-9P*. Negative values for curves indicate that they belong to the turbined water flows and positive values belong to the pumped water flows. Major differences of curves are related to Rio Grande (*RG-TP* and *RG-9P*), while

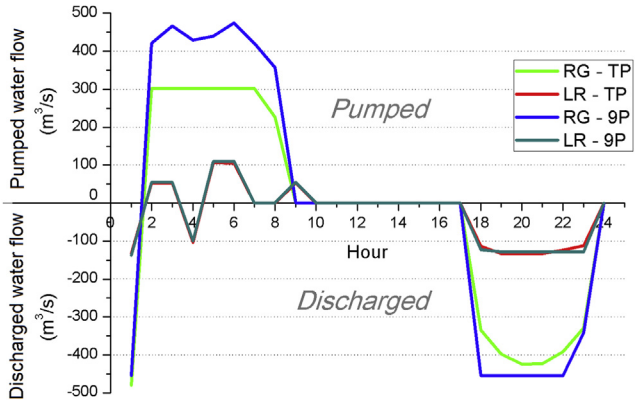

Fig. 9. Comparison between two linear models by considering water discharge and water pumping.

curves for Los Reyunos (*LR-TP* and *LR-9P*) are very similar. It is also of interest to list the total amounts of discharged and pumped flows. Rio Grande pumps 2040 m^3/s water for *TP* model and 3009 m^3/s for *9P* model. The PSHP also discharges 2781 m^3/s for *TP* model and 3075 m^3/s for *9P* model. With regard to Los Reyunos, amounts belonging to the items mentioned above for both models are 370 m^3/s, 383 m^3/s, 984 m^3/s and 1001 m^3/s, respectively.

5. Conclusion

This paper presented a new MILP model that is implemented to determine the optimum operation of Pumped Storage Hydropower Plants (PSHPs). The developed model considers several constraints which are not taken into account in some works, such as the hydraulic head effects for both operating modes. The main difference between the presented linearization technique and other ones, which are available in the literature, is that it allows including an increased number of breakpoints. The greater number of breakpoints distinguishes the proposed model from the classic nine-breakpoint linearization models, and this means obtaining more realistic solutions. In order to prove the effectiveness of the proposed model, two real PSHPs of Argentine Republic are studied. Rio Grande, whose installed capacity is 750 MW and Los Reyunos with an installed capacity of 225 MW. It is important to mention that when it comes to solving the test system by applying the original nonlinear model, feasible solutions cannot be reached within a time limit of 3600 s. Instead, when the test system is solved using the proposed model with a relative gap of 0.05, the optimal solution

Table 6
factor comparison between the two linear models.

Hour	∂_t				Hour	∂_t			
	RG −TP	RG - 9P	LR −TP	LR - 9P		RG −TP	RG - 9P	LR −TP	LR - 9P
1	1.89	7.26	22.64	22.64	13	–	–	–	–
2	29.11	29.11	2.31	2.31	14	–	–	–	–
3	29.11	29.11	2.31	2.31	15	–	–	–	–
4	29.11	29.11	15.44	15.44	16	–	–	–	–
5	29.11	29.11	2.31	2.31	17	–	–	–	–
6	29.11	29.11	2.75	2.75	18	2.37	45.59	–	–
7	29.11	29.11	–	–	19	4.22	22.62	2.85	4.21
8	29.11	29.11	–	–	20	4.36	14.76	22.64	22.64
9	–	–	2.75	2.75	21	4.45	15.21	22.64	22.64
10	–	–	–	–	22	4.08	24.53	22.64	22.64
11	–	–	–	–	23	2.81	17.50	11.65	32.04
12	–	–	–	–	24	–	–	3.16	45.11

is obtained in less than a second of CPU time. To analyze the approximation level of the novel technique, a comparison of three stages between this model and the classical models is performed.

Results indicate that GENCOs in charge of PSHPs take advantage of the energy price variations. In fact, Rio Grande Plant generates 4649 MWh and consumes 4320 MWh. Despite both amounts are very similar, the GENCO obtains a net profit of $99,970 due to the effectiveness of the model. In a similar situation, Los Reyunos obtains a net profit of $69,719, while it generates 1598 MWh and consumes 826 MWh. Results of analyses indicate that the solutions of the new model are more accurate than the solutions of classical methods. The study of power output curves indicates that it fits more closely to the original nonlinear model by up to 15 MWh, in comparison with other linear models. The results of the ∂_t factor show that the new model is almost 19% better than the nine-breakpoint methods. In addition, the analyses of water discharge and water pumping results proves that there are differences up to 969 m^3/s compared with classical models. Over the years, the number of the installed PSHPs is increased at global level. Therefore, optimization tools for operating efficiently these power plants will become increasingly important. The model presented in this work achieves this purpose. Besides the low computation effort that is required for solving the test system, the model can be adapted for the simultaneous operation of a greater number of plants. Moreover, this proposal can be annexed into an economic dispatch problem for solving the power system for the whole country.

Funding

This work was supported by National Scientific and Technical-Research Council (CONICET).

CRediT authorship contribution statement

Gonzalo E. Alvarez: Conceptualization, Methodology, Writing - original draft, Investigation, Software, Validation, Writing - review & editing.

References

[1] International Energy Agency. Global Energy & CO2 Status Report 2018. The latest trends in energy and emissions in 2018. 2019.
[2] Wu Y, Su JR, Li K, Sun C. Comparative study on power efficiency of China's provincial steel industry and its influencing factors. Energy 2019;1009–20. https://doi.org/10.1016/j.energy.2019.03.144.
[3] Khodr HM, Gomez JC, Barinique L, Vivas JH, Paiva P, Yusta JM, et al. A linear programming methodology for the optimization of electric power generation schemes. IEEE Power Eng Rev 2002;22:58. https://doi.org/10.1109/MPER.2002.4312406.
[4] Olabi AG. Renewable energy and energy storage systems. Energy 2017;136:1–6. https://doi.org/10.1016/j.energy.2017.07.054.
[5] Baumann M, Weil M, Peters JF, Chibeles-Martins N, Moniz AB. A review of multi-criteria decision making approaches for evaluating energy storage systems for grid applications. Renew Sustain Energy Rev 2019:516–34. https://doi.org/10.1016/j.rser.2019.02.016.
[6] Rehman S, Al-hadhrami LM, Alam M. Pumped hydro energy storage system : a technological review. Renew Sustain Energy Rev 2015;44:586–98. https://doi.org/10.1016/j.rser.2014.12.040.
[7] International Hydropower Association. Hydropower status report. 2018. 2018.
[8] Ruppert L, Schürhuber R, List B, Lechner A, Bauer C. An analysis of different pumped storage schemes from a technological and economic perspective. Energy 2017;141:368–79. https://doi.org/10.1016/j.energy.2017.09.057.
[9] Cohen AI, Wan SH. An algorithm for scheduling a large pumped storage plant. IEEE Power Eng Rev 1985;5:40. https://doi.org/10.1109/MPER.1985.5526386.
[10] Li Chao-An, Svoboda AJ, Tseng Chung-Li, Johnson RB, Hsu E. Hydro unit commitment in hydro-thermal optimization. IEEE Trans Power Syst 1997;12:764–9. https://doi.org/10.1109/59.589675.
[11] Ghasemi A. Coordination of pumped-storage unit and irrigation system with intermittent wind generation for intelligent energy management of an agricultural microgrid. Energy 2018;142:1–13. https://doi.org/10.1016/j.energy.2017.09.146.
[12] Bozorg Haddad O, Ashofteh P-S, Rasoulzadeh-Gharibdousti S, Mariño MA. Optimization model for design-operation of pumped-storage and hydropower systems. J Energy Eng 2014;140:04013016. https://doi.org/10.1061/(ASCE)EY.1943-7897.0000169.
[13] Finardi EC, Takigawa FYK, Brito BH. Assessing solution quality and computational performance in the hydro unit commitment problem considering different mathematical programming approaches. Elec Power Syst Res 2016;136:212–22. https://doi.org/10.1016/j.epsr.2016.02.018.
[14] Borghetti A, D'Ambrosio C, Lodi A, Martello S. An MILP approach for short-term hydro scheduling and unit commitment with head-dependent reservoir. IEEE Trans Power Syst 2008;23:1115–24. https://doi.org/10.1109/TPWRS.2008.926704.
[15] Narang N, Dhillon JS, Kothari DP. Multiobjective fixed head hydrothermal scheduling using integrated predator-prey optimization and Powell search method. Energy 2012;47:237–52. https://doi.org/10.1016/j.energy.2012.09.004.
[16] Cheng C, Su C, Wang P, Shen J, Lu J, Wu X. An MILP-based model for short-term peak shaving operation of pumped-storage hydropower plants serving multiple power grids. Energy 2018;163:722–33. https://doi.org/10.1016/j.energy.2018.08.077.
[17] Li X, Li T, Wei J, Wang G, Yeh WWG. Hydro unit commitment via mixed integer linear programming: a case study of the three gorges project, China. IEEE Trans Power Syst 2014;29:1232–41. https://doi.org/10.1109/TPWRS.2013.2288933.
[18] Catalao JPS, Mariano SJP, Mendes VMF, Ferreira LAF. Scheduling of head-sensitive cascaded hydro systems: a nonlinear approach. IEEE Trans Power Syst 2009;24:337–46. https://doi.org/10.1109/TPWRS.2008.2005708.
[19] Cheng CT, Cheng X, Shen JJ, Wu XY. Short-term peak shaving operation for multiple power grids with pumped storage power plants. Int J Electr Power Energy Syst 2015;67:570–81. https://doi.org/10.1016/j.ijepes.2014.12.043.
[20] Alvarez GE, Marcovecchio MG, Aguirre PA. Optimization of the integration among traditional fossil fuels, clean energies, renewable sources, and energy storages: an MILP model for the coupled electric power, hydraulic, and natural gas systems. Comput Ind Eng 2020;139:106141. https://doi.org/10.1016/j.cie.2019.106141.
[21] CAMMESA. Report February 2019. https://doi.org/10.18356/fc4b62a8-es. 2019.
[22] Li T, Shahidehpour M. Strategic bidding of transmission-constrained GENCOs with incomplete information. IEEE Trans Power Syst 2005;20:437–47. https://doi.org/10.1109/TPWRS.2004.840378.
[23] NHA - Pumped Storage Development Council. Challenges and opportunities for new pumped storage development. 2012.
[24] Lehtonen E. Production planning of a pumped-storage hydropower plant. MS-E2108 Indep Res Proj Syst Anal 2015;23.
[25] Pirbazari AM. Ancillary services definitions, markets and practices in the world. In: IEEE/PES transm. Distrib. Conf. Expo. Lat. Am., IEEE; 2010; 2010. p. 32–6. https://doi.org/10.1109/TDC-LA.2010.5762857.
[26] Bozorg Haddad O, Ashofteh P-S, Rasoulzadeh-Gharibdousti S, Mariño MA. Optimization model for design-operation of pumped-storage and hydropower systems. J Energy Eng 2014;140:04013016. https://doi.org/10.1061/(asce)ey.1943-7897.0000169.
[27] Paine N, Homans FR, Pollak M, Bielicki JM, Wilson EJ. Why market rules matter: optimizing pumped hydroelectric storage when compensation rules differ. Energy Econ 2014;46:10–9. https://doi.org/10.1016/j.eneco.2014.08.017.
[28] Chen CH, Chen N, Luh PB. Head dependence of pump-storage-unit model applied to generation scheduling. IEEE Trans Power Syst 2017;32:2869–77. https://doi.org/10.1109/TPWRS.2016.2629093.
[29] Ministry of Energy and Mining (MINEM). Inventory of dams and hydroelectric power plants of the Argentine republic. 2016.
[30] Trombotto VG. Rio Grande central hydroelectric complex in pumping accumulation cavern. Energy Report - CNEA 2014;14.
[31] Río EPEC. Grande hydropower plant. 2016.
[32] Ojeda-Esteybar DM, Rubio-Barros RG, Olsina F. Economic and welfare analysis of integrated scheduling of hydrothermal power and natural gas systems: the Argentinian case. In: IEEE PES transm. Distrib. Conf. Exhib. - lat. Am., IEEE; 2018; 2018. p. 1–5. https://doi.org/10.1109/TDC-LA.2018.8511740.
[33] IBM Corp. Ibm. V12. 1: user's manual for CPLEX. Int Bus Mach Corp 2009;12:481.
[34] Diniz AL, Esteves PPI, Sagastizabal CA. A mathematical model for the efficiency curves of hydroelectric units. In: IEEE power eng. Soc. Gen. Meet., IEEE; 2007; 2007. p. 1–7. https://doi.org/10.1109/PES.2007.385632.
[35] Lastusilta T, Bussieck MR, Westerlund T. Comparison of some high-performance MINLP solvers. Chem Eng Trans 2007;11:125–30.